

Cross Dipole Antenna for 4G and Sub-6 GHz 5G Base Station Applications

Geetharamani Gopal¹ and Aathmanesan Thangakalai^{2*}

¹Department of Mathematics
UCE- BIT Campus, Anna University, Tiruchirappalli, Tamilnadu, 620024, India
geetharamani@aubit.edu.in

^{2*}Department of Information and Communication Engineering
UCE- BIT Campus, Anna University, Tiruchirappalli, Tamilnadu, 620024, India
cegnesan@gmail.com

Abstract — Cross dipole antenna for base station applications is presented in this paper. The proposed antenna consists of simple dipole elements and modified balun structure for the improved performance. The proposed design is simple and suitable for 4G and sub-6 GHz 5G base station applications. The antenna is fabricated using low-cost FR4 epoxy substrate with a dielectric permittivity of 4.4. The height of the substrate is 1.6 mm and loss tangent is 0.02. In order to confirm the proposed design, the antenna is measured and compared with the simulation results. The proposed antenna is achieved 13.8 dBi of realized peak gain in the 1.341 to 3.834 GHz frequency range along the bandwidth of 2.492 GHz with VSWR < 1.5. The proposed antenna obtains stable radiation patterns and stable gain over the frequency range. The cross dipole antenna structure with the proper radiation performance makes the proposed antenna suitable for base station applications.

Index Terms — Antennas, base station antenna, cross dipole antenna.

I. INTRODUCTION

Base station antenna is the most important factor in the network coverage of wireless mobile services. There is a demand for base station antenna with a wide frequency band, stable pattern, and high cross polarization ratio. Therefore, in this paper cross dipole antenna for covering 4G and Sub-6 GHz 5G frequency bands is presented. The proposed antenna will offer wideband impedance along with stable gains over the frequency and high polarization ratio. The categories of base station antennae and the design principles are discussed in [1,2]. The basic principles such as wideband impedance, stable patterns in the wide frequency band, high cross polarization ratio in wide-angle range for base station antenna are discussed in [3]. Simulation is playing an increasingly important role in making sure that designs meet specification [4]. Therefore, the

proposed antenna is designed using Finite Integration Technique based tool, which uses the FDTD method for solving Maxwell's equations in grid forms in [5]. The simulation tool, which is selected for this research, is the CST microwave studio. Since features such as antenna matching and integration of circuit elements, multiple antenna systems and phased arrays, installed performance and co-site interference [6] are useful in designing base station antennae. In [7] a wideband differentially fed dual-polarized stacked patch antenna with tuned slots discussed for 1.66 -2.75 GHz having 8.7 dBi gain. In [8] a broadband $\pm 45^\circ$ dual-polarized antenna with y-shaped feeding lines, which operates in 1.7-2.7 GHz frequency with the 8 dBi gain. In [9] a compact broadband dual-polarized antenna array is given for 1.427-2.9 GHz frequency with a gain of 8 dBi. In [10] a wideband omnidirectional antenna array is presented with a low gain variation of 7 ± 1.5 dBi in 1.54-2.75 GHz frequency range. In [11] a low-profile dual-polarized high isolation MIMO antenna arrays for wideband base station applications are discussed for 2.4-3 GHz frequency with 10.2 dBi gain. Broadband stacked f-probe patch antenna and its array for base station are discussed in [12] for 1.7-2.69 GHz frequency having a varying gain of 7.9-8.9 dB. In [13] a low-profile wideband circularly polarized crossed-dipole antenna with wide axial-ratio and gain beam width given for 1-1.68 GHz frequency operation with 5 dBi gain. In [14] surface wave enhanced broadband planar antenna for wireless applications is presented for 3.4-5.5 GHz frequency range with 4.6 dBi gain. In [15] gain enhancement of bow-tie antenna using fractal wideband artificial magnetic conductor ground is discussed for 1.64 – 1.94 GHz frequency range with 6.5 dBi gain. The recent works related to this research is identified in [17-21]. From the literature review, a demand for a single base station antenna to cover a wide frequency range is identified. Therefore, in this paper cross dipole antenna is presented to make stable radiation pattern over the entire frequency range which covers

different wireless mobile communication standards such as 2G, 3G, 4G and the sub-6 GHz 5G applications. The development of the antenna consists of three stages, and initially a single dipole element [16] is designed and its balun structure is modified for the wideband operation next, the two element antenna is developed. Finally, the cross dipole antenna was obtained by the joining of two pairs of dipole structures at the center. At each stage the input matches and radiation parameters are analyzed for the effective progress of the proposed structure. To finish the development process parameters such as input match, radiation patterns, gain, and efficiency are compared for validating the fabricated and simulated antenna structure. The comparison of performance of the proposed antenna with the reference works is also given in the results and discussion part to prove the proposed antenna can serve for base station applications. There are four sections in this paper. An introduction with the literature review in Section 1 and its evolution of design along with the design methodology of the proposed antenna in Section 2. Section 3 consists of a cross dipole antenna and its results. Section 4 concludes the paper.

II. ANTENNA DESIGN

In this section, the design methodology followed in this antenna design is presented. The proposed antenna shown is in Fig. 1. The overall dimension of the single antenna element is $76 \times 42 \text{ mm}^2$. The antenna consists of a simple dipole structure at the top side of the substrate at Fig. 1 (a) and a microstrip balun structure at the bottom side of the rectangular FR4 substrate at Fig. 1 (b). The dimensions for the front view of the antenna consists of, $a=42 \text{ mm}$, $b=76 \text{ mm}$, $c=37.50 \text{ mm}$, $d=23 \text{ mm}$, $e=27 \text{ mm}$, $f=15 \text{ mm}$, $g=1 \text{ mm}$, $h=12.50 \text{ mm}$, $i=11.50 \text{ mm}$, $j=4.50 \text{ mm}$. The FR4 substrate is covered with the double-sided copper cladding with an electrical conductivity of $5.8e+007$ with a thickness of $t=0.035 \text{ mm}$. The evolution of the proposed design is depicted in Fig. 2 and Fig. 3.

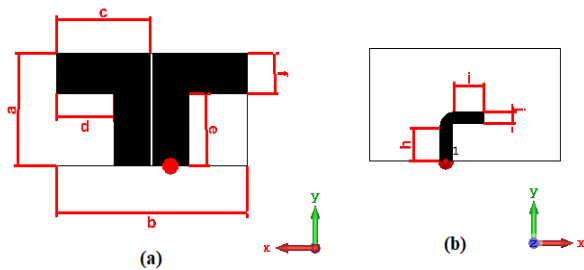


Fig. 1. Geometry of the proposed antenna: (a) top layer and (b) bottom layer.

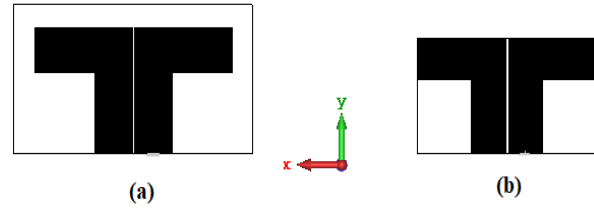


Fig. 2. Evolution of the dipole.

In step 1 a simple dipole of $50 \times 100 \text{ mm}^2$ dimension is designed with the straight balun shown in Fig. 2 (a) which has dual resonant frequencies 1.4 GHz and 2.6 GHz then overall dimension reduced by removal of extra space around the radiating patch following step 2 for size reduction, which is depicted in Fig. 2 (b). It has resulted in the widening of bandwidth from 1.4 GHz to 3.1 GHz. The advantage of using balun is that it acts as an unbalanced to balanced transformer from the feed line to the two printed dipole strips. An integrated balun between the microstrip line and the CPS line to match the input impedance of the antenna to the 50-ohm feed line, and the end of the microstrip line is shorted using a shorting pin at the feeding point is shown in Fig. 2 (a). Step 3 microstrip balun is modified into a curved structure to improve the impedance matching process is shown in Fig. 3 (b).

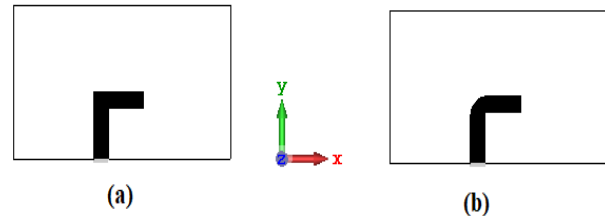


Fig. 3. Evolution of modified balun.

The capacitive gap between the dipole elements is chosen as 1 mm for better isolation between the dipole elements. When the proposed antenna is compared with the traditional dipole antenna with straight balun having narrow bandwidth and the proposed dipole antenna which provides wider bandwidth of 2.64 GHz from 1.30 to 3.94 GHz. Finally, the proposed antenna is obtained with a reduced dimension of $42 \times 76 \text{ mm}^2$. Input match which is obtained during the evolution of design is shown in Fig. 4. The CST software discrete port is used for excitation purposes with the input impedance of 50 ohms.

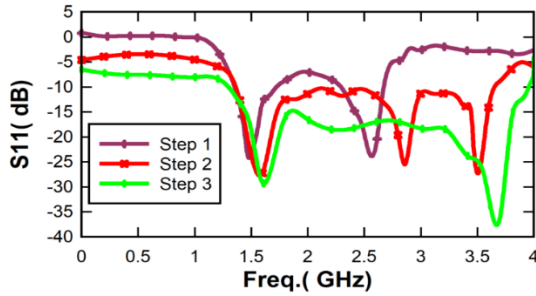


Fig. 4. Input match response to the evolution of design.

III. RESULTS AND DISCUSSION

A. Analysis of single dipole element

The proposed antenna was successfully simulated. Then it is fabricated in 1.6 mm thickness FR4 epoxy substrate with loss tangent $\tan \delta = 0.02$ and dual layer copper with a thickness of 0.035 mm by using a chemical etching method. A photograph of the fabricated prototype antenna is shown in Fig. 5 (a), front view Fig. 5 (b). Back view of the sub-miniature-A (SMA) connector connected to the bottom side for excitation of the antenna. Figure 5 (c) clearly shows the feeding point soldered properly to prevent the outer connector from affecting the balun structure. Hence, it prevents the energy radiated in an expected way. The comparison of simulated and measured S11 values is given in Fig. 6. The return loss ($|S_{11}|$ dB) of the fabricated prototype is measured using the vector network analyzer (Fieldfox RF Analyzer N9912A by Agilent Technologies). It has a bandwidth of 2.64 GHz and VSWR of <1.5 in the same frequency range.

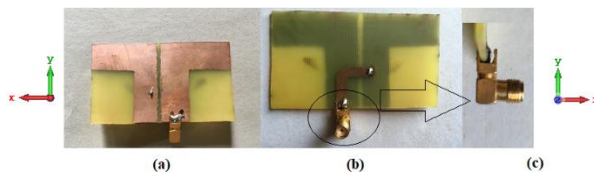


Fig. 5. Prototype of the proposed single element dipole antenna: (a) front view, (b) back view, and (c) feeding point.

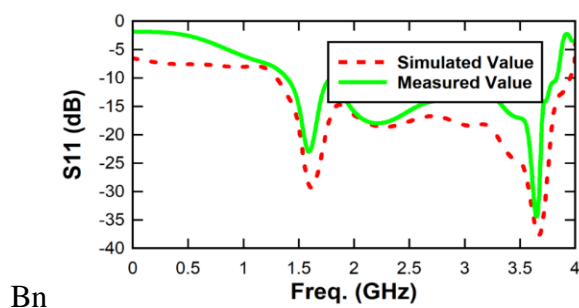


Fig. 6. Comparison of simulated and measured S11.

The values of simulated and measured S11 were close to each other, and the deviations were also observed due to the fabrication process. The surface current is an important variable because it controls the major properties of an antenna such as input impedance, radiation pattern, resonant frequency and bandwidth the simulated surface current distribution is shown in Fig. 7. At Fig. 7 (a) the current flow from the balun to the ends of the dipole resonates with the antenna at the lower bands of frequency. On the other hand, the current distribution is at Fig. 7 (b) is highly dense around the central region of the antenna while a small density among the dipole elements is responsible for the mid-band region. At Fig. 7 (c) the current density is equally spread among the entire resonating elements responsible for the higher bands of frequency. The realized gain vs frequency for single element antenna is given in Fig. 15. Furthermore, the proposed single element antenna finally achieved the realized peak gain of 3 dBi over the frequency band. It is also close to a simulated peak gain of 3.19 dBi.

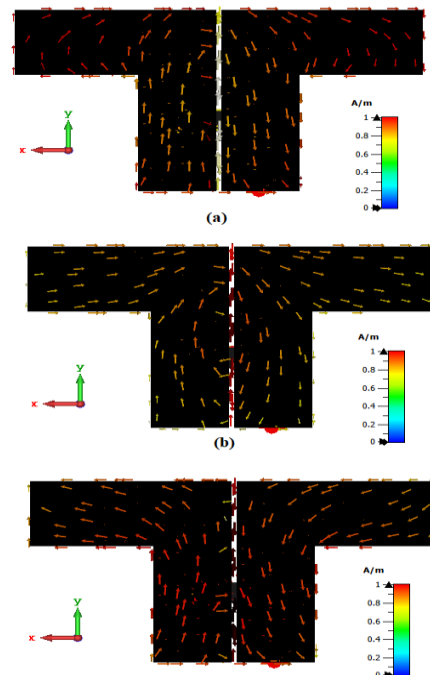


Fig. 7. Surface current distribution: (a) at 1.6 GHz, (b) 2.5 GHz, and (c) 3.8 GHz.

B. Analysis of two element dipole antenna

In order to improve the gain of single element dipole antenna, the two element dipole antenna is developed, and its results are investigated in this section. The proposed two element dipole antenna is shown in Fig. 8. The overall dimension of the proposed two element antenna is $190 \times 42 \text{ mm}^2$. The two dipole antennas are joined together where the distance between the two

dipoles is 38 mm which is chosen as it is half the width of a single dipole antenna. These two dipole antenna elements are fabricated and measured, and their results are discussed. The fabricated prototype of the two element dipole antenna is shown in Fig. 9. The realized gain vs frequency of the two element antenna is shown in Fig. 15. The proposed two element dipole antenna is achieved the stable realized peak gain of 5.8 dBi over the frequency band, it is also like the simulated peak gain of 6.1 dBi. The analysis of the E plane, H plane, Co and Cross polarization of the radiation pattern is important because it gives the overall information on how the antenna radiates in the space.

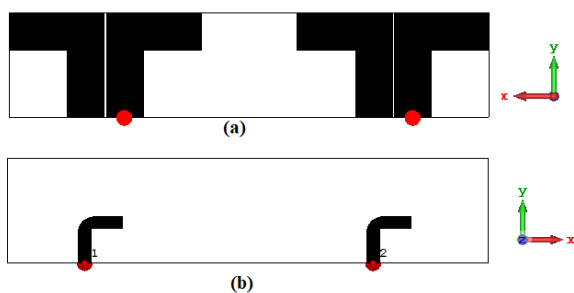


Fig. 8. Two element dipole antenna.



Fig. 9. Fabricated prototype of two element dipole antenna.

Therefore, the radiation pattern is shown in Fig. 10, Fig. 11 for the single and two element antennas at the center frequency of 2.5 GHz. The measured co polarization is 0.153 dBi for single element antenna and for two element antenna it is 3.09 dBi. The cross polarization is -8.35 dBi for single element antenna and for two element antenna it is -12 dBi. The measured radiation efficiency of the single element antenna is found as 82.56% and for the two-element antenna, it is 83.65%.

C. Analysis of cross dipole antenna

The simulated cross dipole antenna is shown in Fig. 12 (a). The balun structure used is shown in Fig. 12 (b). The two element dipole antenna is made a cross by joining at the center of the two elements. The fabricated prototype of the proposed antenna is shown in Fig. 13. The far field radiation patterns such as radiation pattern, gain, and radiation efficiency measurements of the proposed antenna in anechoic chamber. The radiation parameters measured at the center frequency 2.5 GHz are

shown in Fig. 14. The realized peak gain increases to 14.9 dBi during the simulation process and the measured gain is 13.8 dBi. The measured radiation efficiency of the proposed cross dipole antenna is found as 93.25%. The realized gain values for the single, two elements and cross dipole antenna are given in Fig. 15. The stable gain is observed in the frequency range of 1.341-3.834 GHz. The simulated and measured efficiency vs frequency plot is shown in Fig. 16. The stable efficiency is also observed in the frequency range of 1.341-3.834 GHz. In order to know the advantage of the proposed cross dipole antenna, we compare the proposed antennas and the previously reported antennas.

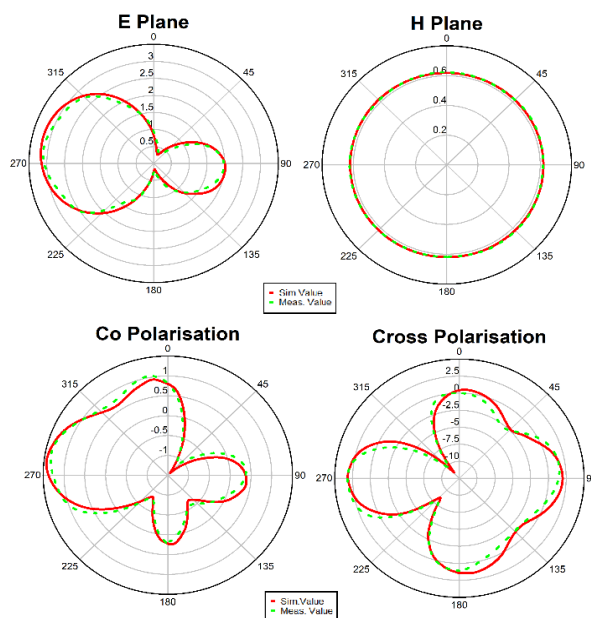


Fig. 10. Radiation patterns of a single element antenna.

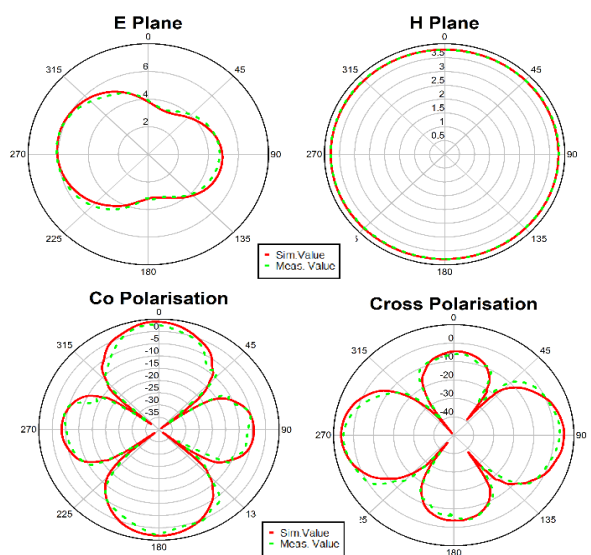


Fig. 11. Radiation patterns of two element antenna.

The comparison for the resonance frequencies, size, substrate material and gains of these antennas is presented in Table 1. From the above discussions, we can see that the proposed antenna is achieved improved bandwidth and gain to cover 4G and sub-6 GHz 5G base station applications.

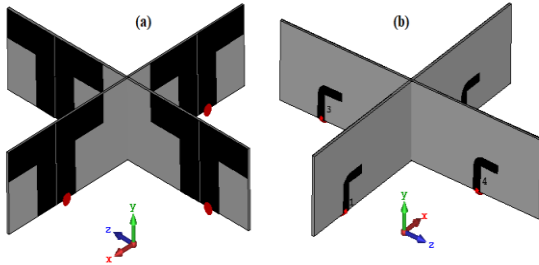


Fig. 12. Simulated cross dipole antenna: (a) dipole elements, and (b) balun structure.

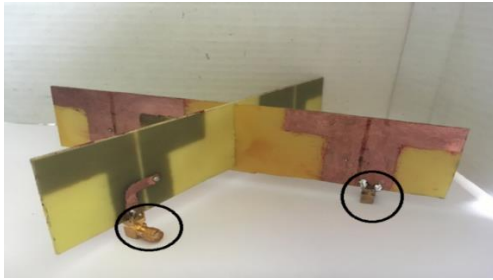


Fig. 13. Fabricated cross dipole antenna.

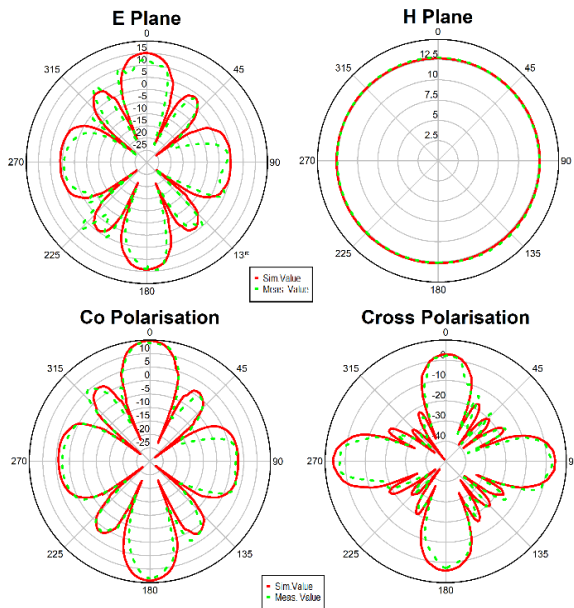


Fig. 14. Radiation patterns of cross element.

Table 1: Comparison between the proposed antenna performance and other reported antennas

Ref.	Frequency (GHz)	Size (mm)	Substrate Material	Gain (dBi)
7	1.66-2.75	140*140	FR4, $\epsilon_r=4.4$, $t=0.8$ mm, loss tangent =0.02	8.7
8	1.7-2.7	140*55*34	FR4, $\epsilon_r=4.4$, $t=0.8$ mm, loss tangent =0.02	8
9	1.427-2.9	990*134.11*33.83	Arlon AD300, $\epsilon_r=3$, $t=0.762$ mm, loss tangent =0.03	8
10	1.54-2.75	63.6*190	FR4, $\epsilon_r=2.55$, $t=1$ mm, loss tangent =0.02	7±1.5
11	2.4-3.00	1112*364*12	FR4, $\epsilon_r=4.4$, $t=3$ mm, loss tangent =0.01	10.2
12	1.7-2.69	460*180*30	FR4, $\epsilon_r=4.4$, $t=1.6$ mm, loss tangent =0.02	7.9-8.9
13	1-1.68	97*81*20.4	FR4, $\epsilon_r=3.38$, $t=0.8$ mm, loss tangent =0.01	5
14	3.4-5.5	60*120	RT Duroid, $\epsilon_r=10.2$, $t=1.27$ mm, loss tangent =0.01	4.6
15	1.64-1.94	70*50*22	FR4, $\epsilon_r=4.4$, $t=3$ mm, loss tangent =0.01	6.5
23	1.64-3.00	100*70*45	FR4, $\epsilon_r=4.4$, $t=0.8$ mm, loss tangent =0.02	6-8
This work	1.341-3.834	190*76*42	FR4, $\epsilon_r=4.4$, $t=1.6$ mm, loss tangent =0.02	13.8

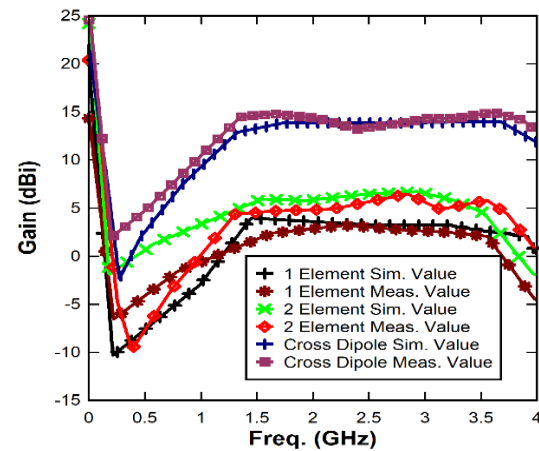


Fig. 15. Realized gain vs Frequency.

The measured co polarization is 6.02 dBi for single element antenna. The cross polarization is -2.98 dBi for the proposed cross dipole antenna. The cross polarization values obtained from the measurement are quite high due to the fabrication tolerance.

The amount of isolation achieved by the proposed antenna is calculated using the parameter Envelope Correlation Coefficient (ECC) which is calculated by using S-parameter coefficients. It is calculated using the equations provided in [22]. The simulated and measured

values of ECC for the cross dipole antenna in Fig. 17. which shows that the ECC values lies below 0.3 makes the proposed antenna is suitable for base station applications.

Simulated 3D Farfield Pattern at 2.5 GHz is shown in Fig. 18 which displays the realized gain pattern at E plane which achieved 14.9 dBi of simulated realized gain.

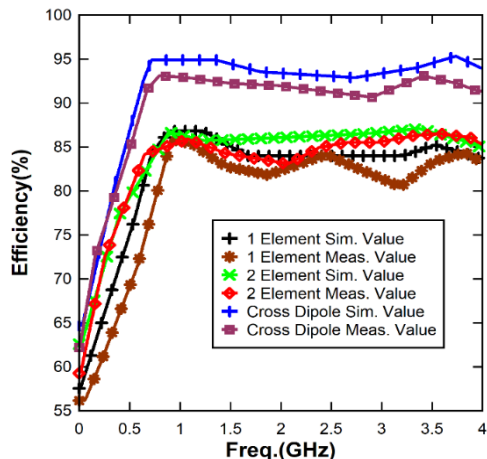


Fig. 16. Efficiency vs. Frequency.

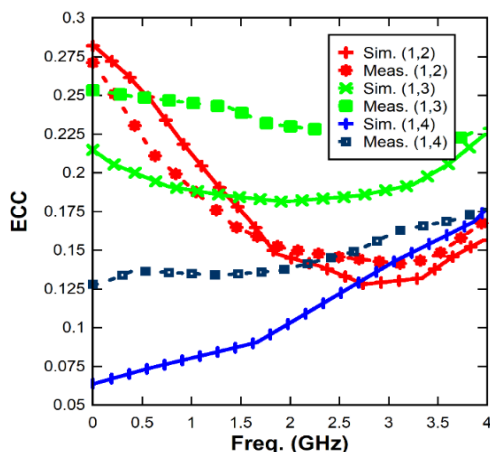


Fig. 17. Simulated and Measured ECC Vs Frequency.

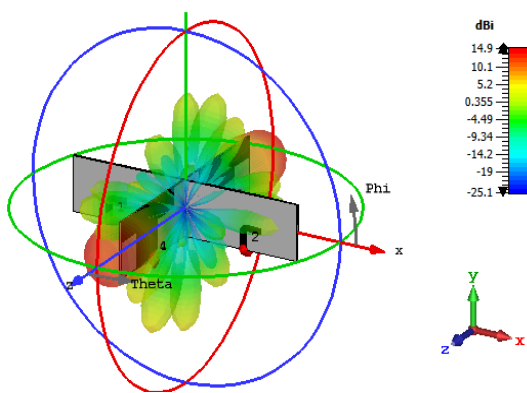


Fig. 18. Simulated 3D Farfield Pattern.

VI. CONCLUSION

In this paper, cross dipole antenna is proposed, and its performance parameters are analyzed and discussed in detail. The antenna operates at 1.341 to 3.834 GHz frequencies with a bandwidth of 2.492 GHz. The proposed antenna is simulated, optimized, fabricated, and measured for the validation of design. The proposed antenna obtains stable radiation patterns and stable gain and also acceptable ECC over the frequency range therefore it is suitable for 4G and sub-6 GHz 5G base station applications.

REFERENCES

- [1] C. A. Balanis, *Antenna Theory: Analysis and Design*, John Wiley & Sons, Singapore, 2005.
- [2] Z. N. Chen and K.-M. Luk, *Antennas for Base Stations in Wireless Communications*, McGraw-Hill Professional, USA, 2009.
- [3] Q. X. Chu, Y. Luo, and D. L. Wen, "Three principles of designing base-station antennas," *International Symposium on Antennas and Propagation (ISAP)*, Hobart, TAS, pp. 1-3, 2015.
- [4] F. Hirtenfelder and J. Mollet, "Phased array simulations using finite integration technique," *JINA Conference*, USA, pp. 1-6, 2004.
- [5] T. Weiland, "RF & microwave simulators - from component to system design," *33rd European Microwave Conference Proceedings (IEEE Cat. No.03EX723C)*, vol. 2, pp. 591-596, 2003.
- [6] M. Rütshlin and T. Wittig, "State of the art antenna simulation with CST studio suite," *9th European Conference on Antennas and Propagation (EuCAP)*, Lisbon, pp. 1-5, 2015.
- [7] Z. Tang, J. Liu, Y. M. Cai, J. Wang, and Y. Yin, "A wideband differentially fed dual-polarized stacked patch antenna with tuned slot excitations," *IEEE Transactions on Antennas and Propagation*, vol. 66, no. 4, pp. 2055-2060, Apr. 2018.
- [8] Q. X. Chu, D. L. Wen, and Y. Luo, "A broadband 45 degree dual-polarized antenna with Y-shaped feeding lines," *IEEE Transactions on Antennas and Propagation*, vol. 63, no. 2, pp. 483-490, Feb. 2015.
- [9] Q. Zhang and Y. Gao, "A compact broadband dual-polarized antenna array for base stations," *IEEE Antennas and Wireless Propagation Letters*, vol. 17, no. 6, pp. 1073-1076, June 2018.
- [10] Y. Yu, J. Xiong, and R. Wang, "A wideband omnidirectional antenna array with low gain variation," *IEEE Antennas and Wireless Propagation Letters*, vol. 15, pp. 386-389, Dec. 2016.
- [11] H. Zhai, L. Xi, Y. Zang, and L. Li, "A low-profile dual-polarized high-isolation MIMO antenna arrays for wideband base-station applications," *IEEE Transactions on Antennas and Propagation*,

- vol. 66, no. 1, pp. 191-202, Jan. 2018.
- [12] Y. Jin and Z. Du, "Broadband stacked f-probe patch antenna and its array for base station," *IEEE International Wireless Symposium*, Shenzhen, pp. 1-4, 2015.
- [13] W. J. Yang, Y. M. Pan, and S. Y. Zheng, "A low-profile wideband circularly polarized crossed-dipole antenna with wide axial-ratio and gain beamwidths," *IEEE Transactions on Antennas and Propagation*, vol. 66, no. 7, pp. 3346-3353, July 2018.
- [14] K. M. K. H. Leong, Y. Qian, and T. Itoh, "Surface wave enhanced broadband planar antenna for wireless applications," *IEEE Microwave and Wireless Components Letters*, vol. 11, no. 2, pp. 62-64, Feb. 2001.
- [15] Y. W. Zhong, G. M. Yang, and L. R. Zhong, "Gain enhancement of bow-tie antenna using fractal wideband artificial magnetic conductor ground," *Electronics Letters*, vol. 51, no. 4, pp. 315-317, 2015.
- [16] A. Kashkool, S. Yahya, H. Al-Rizzo, A. Al-Wahhamy, and A. A. Issac, "On the design and simulation of antennas on ultra-thin flexible substrates," *ACES Journal*, vol. 33, no. 7, pp. 798-801, July 2018.
- [17] L.-Y. Chen, J.-S. Hong, and M. Amin, "A compact CPW-fed MIMO antenna with band-notched characteristic for UWB system," *ACES Journal*, vol. 33, no. 7, pp. 818-821, July 2018.
- [18] Z. Liu, Y. Li, J. Liu, Y. Zhang, X. Wu, and Y. Zhou, "A broadband dual-polarized antenna for TD-SCDMA system," *ACES Journal*, vol. 32, no. 12, pp. 1121-1124, Dec. 2017.
- [19] V. Rafiei, H. Saygin, and S. Karamzadeh, "Circularly polarized aperture-coupled microstrip-line fed array antenna for WiMAX/C bands applications," *ACES Journal*, vol. 32, no. 12, pp. 1117-1120, Dec. 2017.
- [20] M. Sierra-Castañer, "Review of recent advances and future challenges in antenna measurement," *ACES Journal*, vol. 33, no. 1, pp. 99-102, Jan. 2018.
- [21] R. L. Li, B. Pan, T. Wu, K. Lim, J. Laskar, and M. M. Tentzeris, "A broadband printed dipole and a printed array for base station applications," 2008 *IEEE Antennas and Propagation Society International Symposium*, San Diego, CA, pp. 1-4, 2008.
- [22] S. Chouhan, D. K. Panda, M. Gupta, and S. Singhal, "Multiport MIMO antennas with mutual coupling reduction techniques for modern wireless transceive operations: A review," *Int. J. RF Microw. Comp. Aided Engg.*, 2017.
- [23] S. X. Ta, C. D. Bui, and T. K. Nguyen, "Wideband quasi-yagi antenna with broad-beam dual-polarized radiation for indoor access points," *ACES Journal*, vol. 34, no. 5, pp. 654-660, May 2019.



Geetharamani. G is working as an Associate Professor in Department of Mathematics, UCE BIT Campus, Anna University, Trichy. She received her Ph.D in Gandhigram Rural University. She received M.E. (CSE) in Anna University, Chennai. She received M.Phil in National College, Trichy, She received M.Sc. in Bharathidasan University. She received PGDCA in Alagappa University.



Aathmanesan. T pursuing Ph.D. in Anna University, He received his M.Tech. degree in College of Engineering Guindy, Anna University Chennai. He completed his B.E. ECE in Anna University Chennai. His area of research are microwave and THz antennas.